Quantum Hall Effect in n-p-n and n-2D Topological Insulator-n Junctions

G. M. Gusev,[1] A. D. Levin,[1] Z. D. Kvon,[2] N. N. Mikhailov,[2] and S. A. Dvoretsky[2]

[1]Instituto de Física da Universidade de São Paulo, 135960-170 São Paulo, SP, Brazil
[2]Institute of Semiconductor Physics, Novosibirsk 630090, Russia

(Received 11 October 2012; published 14 February 2013)

We have studied quantized transport in HgTe wells with inverted band structure corresponding to the two-dimensional topological insulator phase (2D TI) with locally controlled density allowing n-p-n and n-2D TI-n junctions. The resistance reveals the fractional plateau $2h/e^2$ in the n-p-n regime in the presence of the strong perpendicular magnetic field. We found that in the n-2D TI-n regime the plateaux in resistance in not universal and results from the edge state equilibration at the interface between chiral and helical edge modes. We provided the simple model describing the resistance quantization in n-2D TI-n regime.

DOI: 10.1103/PhysRevLett.110.076805 PACS numbers: 73.43.Fj, 73.23.−b, 85.75.−d

Recently, interest in edge state transport in the integer quantum Hall effect (QHE) has been renewed due to observation of the conductance quantization in the locally gated graphene layers in the bipolar regime [1–3]. It has been demonstrated that the density variation across the charge neutrality point results in a p-n junction with interesting transport properties that are absent in the QHE regime in the unipolar case. In particular, the two-terminal resistance reveals fractional quantization in the graphene p-n [1] or n-p-n [2,3] junctions, which has been attributed to chiral edge states equilibration at the p-n interfaces [4]. In general, the character of the QHE transport in unipolar and bipolar regimes is quite different. In the unipolar regime the edge states propagate in the same direction [Fig. 1(a)], while in the bipolar regime the edge states countercirculate in the p and n regions, propagating parallel to each other along the interface [Fig. 1(c)]. The intermode scattering across the interface in the presence of the disorder leads to interference between channels, and conductance should exhibit fractional quantization superimposed by universal conductance fluctuations (UCF) [4].

Note, however, that UCF in the bipolar regime have not been observed, which has been attributed to several extrinsic and intrinsic mechanisms [4]. Further study demonstrated that UCF in a sufficiently small (mesoscopic) system are robust to sample disorder [5], but could be suppressed in the absence of the intervalley scattering [6]. In the latter case, the plateaux value is expected to be shifted up or down from the quantized value, which disagrees with experiments. Therefore, the microscopic mechanism providing plateaux quantization in graphene p-n and p-n-p structures still remains unclear. The semiclassical approach [7] confirms this conclusion.

Another interesting system, which provides for realization of the p-n junction and study of the QHE in the bipolar regime, is the HgTe-based quantum well. The transport properties of such a system depends on the well width d. In particular, when d exceeds the "critical" width approximately equal to 6.3 nm, the energy spectrum becomes inverted and one changes to a two-dimensional topological insulator (2D TI), or quantum spin Hall insulator phase (QSHI) characterized by an insulating gapped

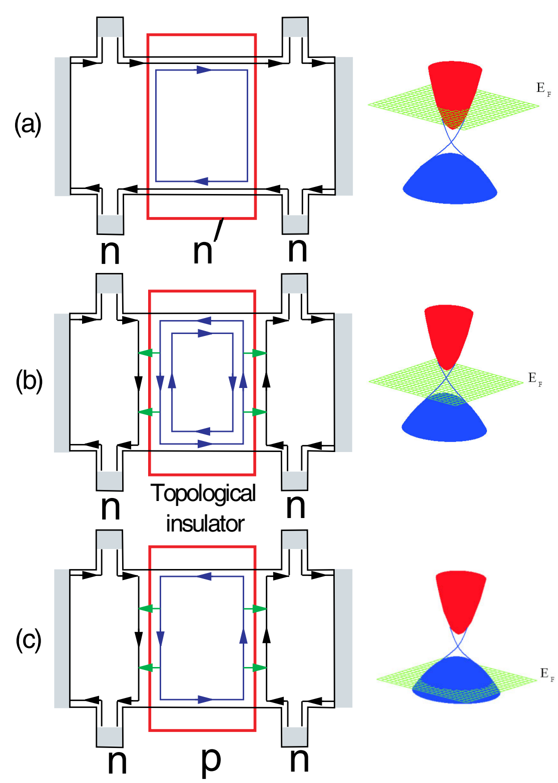

FIG. 1 (color online). Schematics of edge state propagation for different charge densities in the central local gate region (red rectangular) and in the regions outside the local gate in the strong magnetic field: (a) n-n'-n junction, $n' > n$, (b) n-2DTI-n junction, (c) n-p-n junction $n = p$, where n (p) refers to negative (positive) charge density. Insets—the energy spectrum for different Fermi energy positions in the region under local gate at $B = 0$.

phase in the bulk and conducting edge modes, which propagate along the sample periphery [8–13]. As in graphene, both the carrier type and density in the HgTe-based well can be electrostatically controlled via the employment of the global or local gate [14]. Moreover, when the ungated HgTe well is initially n-doped, the realization of n-p or n-p-n junction requires only a single local gate in contrast to graphene, where a combination of the local and global control of the carrier type and density is necessary [1–3].

In the present Letter, we report the realization of local top gating in a HgTe-based quantum well with inverted band structure for which the density in each region could be varied across the gap, allowing a n-p-n junction to be formed at the interfaces. Moreover, when the Fermi energy in the region under the local gate lies in the bulk gap band, the transport at the junction interface is described by mode mixing between conventional QHE edge channels and pairs of counter-propagating modes with opposite spin polarizations [Fig. 1(b)], corresponding to QSHI. We find the fractional quantum Hall effect plateaux $R = 2\frac{h}{e^2}$ in the n-p-n regime in accordance with a mode describing the countercirculate mixing edge state model [3,4]. Surprisingly, we did not find mesoscopic conductance fluctuations, although our samples were sufficiently small and transport would be expected to be coherent. In the n-QHSI-n regime resistance reveals quantization close to the $1.3\frac{h}{e^2}$ value, which clearly demonstrates the existence of the countercirculating edge states in the bulk gap region.

The $Cd_{0.65}Hg_{0.35}Te/HgTe/Cd_{0.65}Hg_{0.35}Te$ quantum wells with (013) surface orientations and a width d of 8 nm were prepared by molecular beam epitaxy. A detailed description of the sample structure has been given in Refs. [15,16]. The six-probe Hall bar was fabricated with a lithographic length of 6 μm and width of 5 μm. The Ohmic contacts to the two-dimensional gas were formed by inburning of indium. To prepare the gate, a dielectric layer containing 100 nm SiO_2 and 200 nm Si_3Ni_4 was first grown on the structure using the plasmochemical method. Then, the TiAu gate with a width of $W = 2 - 3$ μm was deposited. Width W is smaller than the distance between potentiometric probes; therefore, the voltage applied to this local gate tunes the density only in the strip below the gate and creates a tunable potential barrier (see Fig. 2). The ungated HgTe well was initially n doped with density $n_s = 1.8 \times 10^{11}$ cm^{-2}. Several devices with the same configuration have been studied. The density variation with gate voltage was 1.09×10^{15} m^{-2}V^{-1}. For comparison, we also used a device with the gate covering all the sample area including the potentiometric probes, dedicated for conventional 4-probe measurements [inset to Fig. 2(b)]. The magnetotransport measurements in the structures described were performed in the temperature range 1.4–25 K and in magnetic fields up to 12 T using a standard four point circuit with a 3–13 Hz ac current of 0.1–10 nA through the sample, which is sufficiently low to avoid overheating effects.

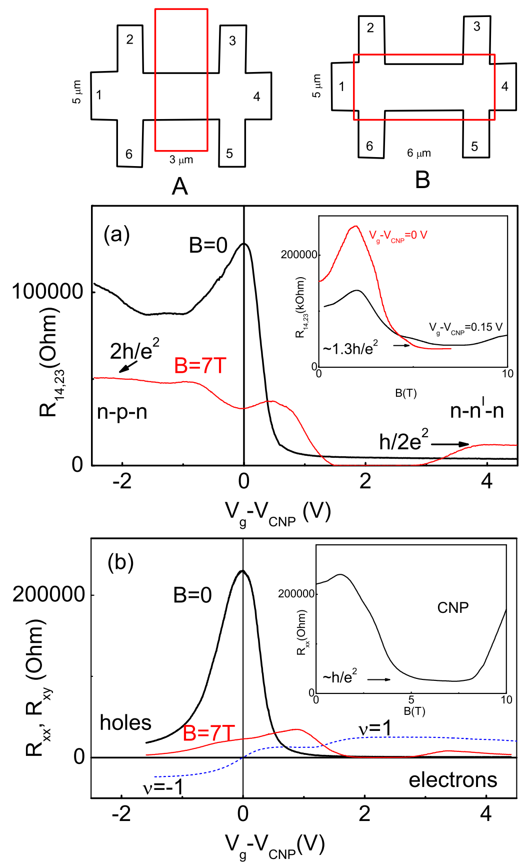

FIG. 2 (color online). (a) The longitudinal $R_{14,23}$ ($I = 1, 4$; $V = 3, 2$) resistance as a function of the gate voltage at zero magnetic field (black thick line) and $B = 7$ T (thin red line) in the local gate sample, labeled A; $T = 1.4$ K. The inset shows the magnetic field dependence for two gate voltages. (b) The longitudinal R_{xx} ($I = 1, 4$; $V = 3, 2$) resistance as a function of the gate voltage at zero magnetic field (black thick line) and $B = 7$ T (thin red line), and Hall R_{xy} ($I = 1, 4$; $V = 2, 6$) resistances in the global gate sample labeled B; $T = 1.4$ K. The inset shows the magnetic field dependence near CNP. The top panel shows the schematics view of the samples. The perimeter of the gate is shown by the rectangle.

The density of the carriers in the HgTe quantum wells can be electrically manipulated with local gate voltage V_g. The typical dependence of the four-terminal $R_{14,23} = R_{I=1,4;V=2,3}$ resistance of one of the representative samples as a function of V_g is shown in Fig. 2. The resistance $R_{14,23}$ in a zero magnetic field exhibits a sharp increase when the electrochemical potential enters the insulating bulk gap and reaches saturation at a level that is ~10 times greater than the universal value $h/2e^2$, which is expected for the 2D TI phase. This value varies from 150 to 300 kOhm in different samples. The device with a global gate reveals a sharp peak, shown in Fig. 2(b), when the gate voltage induces an additional charge density, altering the quantum wells from an n-type conductor to a p-type conductor via a QSHI state. It has been shown [12,13] that the 4-probe resistance in an HgTe/CdTe micrometer-sized ballistic Hall bar demonstrated a quantized plateaux $R_{14,23} \simeq h/2e^2$. It is expected that the stability of the helical edge states in the topological insulator is unaffected by the presence of a weak disorder [8–10]. Note, however, that quantized ballistic transport has been observed only in micrometer-sized samples, and the plateaux $R_{14,23} \simeq h/2e^2$ is destroyed if the sample is above a certain critical size of about a few microns [12,17]. The understanding of the stability of the plateaux in macroscopic samples requires further investigation. The Hall effect reverses its sign and $R_{xy} \approx 0$ when R_{xx} approaches its maximum value [Fig. 2(b)], which can be identified as the charge neutrality point (CNP). These behaviors resemble the ambipolar field effect observed in graphene [18]. Application of the perpendicular magnetic field leads to suppression of the peak in both structures, although the behavior of the resistance in the electron and hole parts of the spectrum is quite different. One can see that the resistance in a local gate device shows the plateaus $R_{14,23} \approx 2\frac{h}{e^2}$ in the n-p-n region and $R_{14,23} \approx \frac{1}{2}\frac{h}{e^2}$ in the n-n'-n region, while the device with a global gate demonstrates conventional quantum Hall behaviour. Note also that $R_{14,23} = 0$ near $V_g - V_{\rm CNP} \approx 2V$ in both structures. Figure 3 shows the resistance of the local gate device in the voltage-magnetic field plane. One can see the evolution of the longitudinal resistance

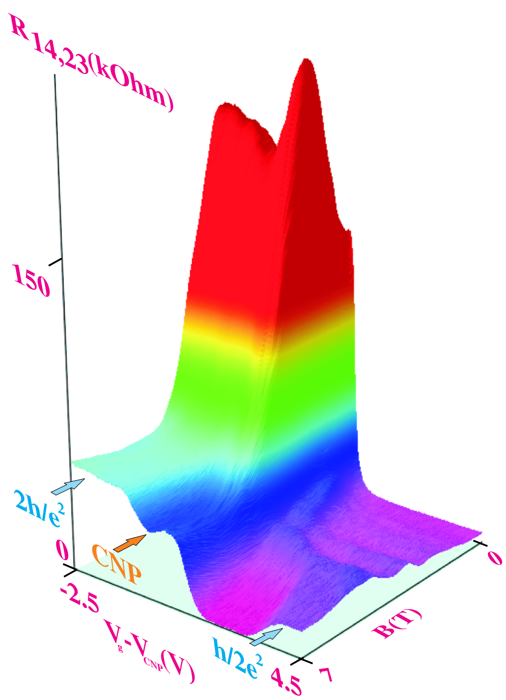

FIG. 3 (color online). The longitudinal resistance $R_{14,23}$ as a function of the gate voltage and magnetic field, $T = 1.4$ K. Two plateaux $R_{14,23} \approx 2\frac{h}{e^2}$ and $R_{14,23} \approx \frac{1}{2}\frac{h}{e^2}$ are indicated by blue arrows. CNP is indicated by the orange arrow.

with the magnetic field and density in the n-p-n, n-n'-n and n-TI-n regions. The resistance peak drops dramatically in a magnetic field above 3 T and shows plateauxlike behaviour $R_{14,23} \approx 2\frac{h}{e^2}$ in the $B - V_g$ plane in the n-p-n region. Such resistance decrease demonstrates the transition to the edge state transport regime. This behavior can be understood from quasi classical picture: Lorentz force push one of the electron trajectory forward to the edge, while other one, which is propagating in opposite direction, is declined from the edge. Since the distance between trajectories increases, it may lead to the suppression of the scattering between channels. For positive gate voltage ($V_g - V_{\rm CNP} > 3.5$ V), when n-n'-n junctions are expected to be formed, one can see a series of the fully developed plateaux with magnetic field. As B increases, the final plateaux $R_{14,23} \approx \frac{1}{2}\frac{h}{e^2}$ emerges. Similar behaviour is observed around CNP, when the QSHI phase is formed under local gate, the plateaux $R_{14,23} \approx 1.3\frac{h}{e^2}$ develops in a wide range of the magnetic field [see inset to Fig. 2(a)] and narrow range of density. Slightly above CNP, in the electronic part of the peak, the resistance value is shifted up and approaches the value $R_{14,23} \approx 1.43\frac{h}{e^2}$. In the region between this plateaux and $R_{14,23} \approx \frac{1}{2}\frac{h}{e^2}$, the resistance vanishes and shows pronounced minima. In the rest of the Letter, we will focus on the explanation of the resistance quantization in HgTe quantum wells in the bipolar regime in a strong magnetic field.

QHE edge state transport in the Hall bar geometry with a gate finger across the device has been extensively explored in the past in the monopolar regime [19]. The 4-probe resistance is expected to be quantized at values $R_{14,23} = \frac{h}{e^2}(\frac{1}{\nu} - \frac{1}{\nu_g})$, where ν_g is the Landau level filling factor in the gate region, and ν is the filling factor in the region outside of the gate. Indeed, this formula perfectly describes the resistance behavior at $V_g - V_{\rm CNP} > 0$ in a magnetic field above 3 T, notably. $R_{14,23} = \frac{h}{e^2}(\frac{1}{1} - \frac{1}{1}) = 0$ and $R_{14,23} = \frac{h}{e^2}(\frac{1}{1} - \frac{1}{2}) = \frac{1}{2}\frac{h}{e^2}$.

In the bipolar regime, an unusual fractional resistance plateaux arises from the equilibration between countercirculating edge states in the p and n regions [see Fig. 1(c)] [4]. In the 2-probe configuration, the net resistance is described by three quantum resistors in series: $R_{2T} = \frac{h}{e^2}(\frac{1}{\nu} + \frac{1}{\nu_g} + \frac{1}{\nu}) = \frac{h}{e^2}\frac{2\nu+\nu_g}{\nu_g\nu}$, which indeed has been observed in graphene n-p-n junctions [3]. The quantization of the 4-probe resistance is given by a slightly different equation, $R_{4T} = R_{14,23} = \frac{h}{e^2}(\frac{1}{\nu} + \frac{1}{\nu_g})$. This formula agrees with our observation of plateaux $R_{14,23} = \frac{h}{e^2}(\frac{1}{1} + \frac{1}{1}) = 2\frac{h}{e^2}$ in the n-p-n regime [Figs. 2(a) and 3]. It is worth noting that in graphene it is difficult to obtain the plateau at this value, since the valley and spin splitting is small and $\nu = \nu_g = \pm 2, \pm 6 \ldots$. The advantage of the graphene structure is the sharper (but not abrupt) potential step on the scale of the magnetic length [3].

A more interesting situation occurs when the Fermi energy in the region under the local gate tunes through the 2D TI phase [Fig. 1(b)]. Such a situation allows us to use QHE mode propagation for investigation of the intrinsic transport characteristics of the topological insulator. As mentioned above, the gaplessness of the edge states in TI is protected against time reversal symmetry (TRS), which must result in the robust ballistic transport. However, a magnetic field perpendicular to the 2D layer breaks the TRS and thereby enables elastic scattering between counterpropagating chiral edge states. A number of different conflicting scenarios have been developed for TRS breaking in the QSHI system [12,20,21]. The more realistic models [20,21] have demonstrated that the counterpropagating helical edge states persist in a strong B. The magnetic field does not affect the gap but it modifies the energy spectrum of the edge states and generates backscattering between the counterpropagating modes [20]. However, the model did not present any realistic description of the scattering and can hardly be compared with experimental observations. Model [22] predicted that in magnetic fields above critical value (B_c), the band structure becomes normal and one enters the ordinary insulator regime. The critical magnetic field was estimated and was found for HgTe devices $B_c \approx 7.4$ T; therefore, the resistance increase above 7 T (insets to Fig. 2) can be attributed to the TI- ordinary insulator transition.

In n-2D TI-n regime one of the helical modes propagates in the same direction as the edge state outside of the gate, while the other has the opposite direction and, therefore, flows parallel to the outside mode [Fig. 1(b)]. The edge modes are described by the local chemical potentials ξ, φ, and ψ, where φ and ψ are electrochemical potentials for counterpropagating TI states and ξ is conventional quantum Hall effect potential outside of the gate region [23]. We can introduce phenomenological constant γ, which represent spin flip scattering between modes φ and ψ. The scattering between conventional QHE edge mode ξ and helical modes φ and ψ is characterized by 2 parameters, λ and β, consequently. The edge state transport can be described by equations for particle density [24,25], taking into account the scattering between edge modes [23]. The model reproduces the near quantized value of the resistance $R_{14,23} \approx 1.3\frac{h}{e^2}$ with 3 parameters $\lambda = 0.8\ \mu\mathrm{m}^{-1}$, $\beta = 0.5\ \mu\mathrm{m}$ and $\gamma = 0.27\ \mu\mathrm{m}^{-1}$. Indeed, our model correctly reproduces the value of the resistance $R_{14,23} \approx 2\frac{h}{e^2}$ for $\gamma \approx 0$, which corresponds to the n-p-n situation [Fig. 1(c)]. One can see that all deduced parameters have close values, since the spin flip scattering is strong in the presence of the Rashba interaction [26], and transition between spin polarized states is qualitatively similar to transition between spin degenerate modes.

We note that the parameter γ can be independently obtained from the measurements in the global gate sample. The 4-terminal resistance is not universal in the presence of the backscattering and can be described by transport equations [23] similar to the local gate case. We performed numerical calculations for counterpropagating potentials in the global gate sample and found resistance. Our calculations reproduced the value $R_{xx} \approx h/e^2$, which has been observed in experiment at $B = 7$ T [inset to Fig. 2(b)] with parameter $\gamma \approx 0.27\ \mu\mathrm{m}^{-1}$ in agreement with the previous situation. Therefore, the plateaux-like behaviour of the resistance unambiguously demonstrates the existence of the counter circulating modes, when the Fermi level tunes through the bulk gap. Our observation provides considerable support for the models [20,21], which predict persistence of the helical modes in a strong magnetic field. In our model, the resistance value exceeds h/e^2 for any the parameters of the backscattering between modes.

We also measured the temperature dependence of the resistance in all regimes and found that all plateaus remain unchanged when the temperature decreases from 10 to 1.4 K. In the coherent regime for small enough samples, the theory [4] predicts UCF in bipolar structures. We expected the coherence length in our samples to be of the order of $\sim 1\ \mu$m at 1.4 K [27] and, therefore, UCF in our samples could be not completely suppressed. However, similarly to the graphene n-p-n junction, we did not observe UCF as a function of Fermi energy or magnetic field either in n-p-n or in n-2D TI-n regimes.

In conclusion, we have studied the transport properties of the HgTe-based quantum well with inverted band structure with a gate finger located across the Hall bar geometry in a strong magnetic field. The narrow gap band structure of HgTe allows local gate field control of the carrier type and density, and hence, the creation of a bipolar n-p-n junction within a single quantum well. We observed a fractional resistance plateau $2h/e^2$ originating from the mixing of modes at the p-n interfaces. By varying the voltage on the local gate, we studied the QHE transport in the n-2D TI-n regime, where two counterpropagating helical modes circulate along the junction interface. The intermode scattering between helical states and the QHE chiral edge mode results in resistance quantization at a value $R_{14,23} \approx 1.3\frac{h}{e^2}$. This effect can be used to explore the backscattering mechanism in a 2D topological insulator. Our observations support the model that predicts the robustness of helical modes in the presence of a perpendicular magnetic field [20].

We thank O. E. Raichev for helpful discussions. The financial support of this work by FAPESP, CNPq (Brazilian agencies), RFBI and RAS programs "Fundamental researches in nanotechnology and nanomaterials" and "Condensed matter quantum physics" is acknowledged.

[1] J. R. Williams, L. DiCarlo, and C. M. Marcus, Science **317**, 638 (2007).

[2] B. Huard, J. A. Sulpizio, N. Stander, K. Todd, B. Yang, and D. Goldhaber-Gordon, Phys. Rev. Lett. **98**, 236803 (2007).

[3] B. Özyilmaz, P. Jarillo-Herrero, D. Efetov, D. A. Abanin, L. S. Levitov, and P. Kim, Phys. Rev. Lett. **99**, 166804 (2007).
[4] D. A. Abanin and L. S. Levitov, Science **317**, 641 (2007).
[5] W. Long, Q. F. Sun, and J. Wang, Phys. Rev. Lett. **101**, 166806 (2008).
[6] J. Tworzydło, I. Snyman, A. R. Akhmerov, and C. W. J. Beenakker, Phys. Rev. B **76**, 035411 (2007).
[7] P. Carmier, C. Lewenkopf, and D. Ullmo, Phys. Rev. B **84**, 195428 (2011).
[8] C. L. Kane and E. J. Mele, Phys. Rev. Lett. **95**, 146802 (2005).
[9] B. A. Bernevig, T. L. Hughes, and S. C. Zhang, Science **314**, 1757 (2006).
[10] M. Z. Hasan and C. L. Kane, Rev. Mod. Phys. **82**, 3045 (2010); X.-L. Qi and S.-C. Zhang, Rev. Mod. Phys. **83**, 1057 (2011).
[11] X.-L. Qi and S.-C. Zhang, Phys. Today **63**, No. 1, 33 (2010).
[12] M. König, S. Wiedmann, C. Brune, A. Roth, H. Buhmann, L. W. Molenkamp, X.-L. Qi, and S.-C. Zhang, Science **318**, 766 (2007).
[13] H. Buhmann, J. Appl. Phys. **109**, 102409 (2011).
[14] G. M. Gusev, E. B. Olshanetsky, Z. D. Kvon, N. N. Mikhailov, S. A. Dvoretsky, and J. C. Portal, Phys. Rev. Lett. **104**, 166401 (2010); G. M. Gusev, E. B. Olshanetsky, Z. D. Kvon, A. D. Levin, N. N. Mikhailov, and S. A. Dvoretsky, Phys. Rev. Lett. **108**, 226804 (2012).
[15] Z. D. Kvon, E. B. Olshanetsky, D. A. Kozlov N. N. Mikhailov, and S. A. Dvoretsky, Pis'ma Zh. Eksp. Teor. Fiz. **87**, 588 (2008) [JETP Lett. **87**, 502 (2008)].
[16] E. B. Olshanetsky, Z. D. Kvon, N. N. Mikhailov, E. G. Novik, I. O. Parm, and S. A. Dvoretsky, Solid State Commun. **152**, 265 (2012).
[17] G. M. Gusev, Z. D. Kvon, O. A. Shegai, N. N. Mikhailov, S. A. Dvoretsky, and J. C. Portal, Phys. Rev. B **84**, 121302 (R) (2011).
[18] S. D. Sarma, S. Adam, E. H. Hwang, and E. Rossi, Rev. Mod. Phys. **83**, 407 (2011).
[19] R. J. Haug, Semicond. Sci. Technol. **8**, 131 (1993).
[20] G. Tkachov and E. M. Hankiewicz, Phys. Rev. Lett. **104**, 166803 (2010).
[21] J. Maciejko, X.-L. Qi, and S.-C. Zhang, Phys. Rev. B **82**, 155310 (2010).
[22] B. Scharf, A. Matos-Abiague, and J. Fabian, Phys. Rev. B **86**, 075418 (2012).
[23] See Supplemental Material at http://link.aps.org/supplemental/10.1103/PhysRevLett.110.076805 for details on the model taking into account the edge state contribution to the total current near CNP.
[24] D. A. Abanin, K. S. Novoselov, U. Zeitler, P. A. Lee, A. K. Geim, and L. S. Levitov, Phys. Rev. Lett. **98**, 196806 (2007).
[25] V. T. Dolgopolov, G. V. Kravchenko, and A. A. Shashkin, Solid State Commun. **78**, 999 (1991); V. T. Dolgopolov, A. A. Shashkin, G. M. Gusev, and Z. D. Kvon, Pis'ma Zh. Eksp. Teor. Fiz. **53**, 461 (1991) [JETP Lett. **53**, 484 (1991)].
[26] A. V. Khaetskii, Phys. Rev. B **45**, 13777 (1992).
[27] E. B. Olshanetsky, Z. D. Kvon, G. M. Gusev, N. N. Mikhailov, S. A. Dvoretsky, and J.-C. Portal, JETP Lett. **91**, 347 (2010).